

1 **Glucocorticoid treatment exacerbates mycobacterial infection by
2 reducing the phagocytic capacity of macrophages**

3 **Glucocorticoids and zebrafish TB**

4 Yufei Xie, Annemarie H. Meijer, Marcel J.M. Schaaf*

5 Institute of Biology, Leiden University, Leiden, The Netherlands

6

7 * To whom correspondence should be addressed. Tel: (+31)715274975; Fax: (+31)715275088; Email:
8 m.j.m.schaaf@biology.leidenuniv.nl

9

10 **Key words:** glucocorticoids, *Mycobacterium marinum*, macrophage, phagocytosis, zebrafish,
11 tuberculosis

12

13 **Summary statement:**

14 Using a zebrafish tuberculosis model, we show that glucocorticoids decrease phagocytosis by
15 macrophages, thereby increasing the bacterial burden. This may explain the glucocorticoid-induced
16 increase in susceptibility to tuberculosis in humans.

17 Abstract

18 Glucocorticoids are effective drugs for treating immune-related diseases, but prolonged therapy is
19 associated with an increased risk of various infectious diseases, including tuberculosis. In this study,
20 we have used a larval zebrafish model for tuberculosis, based on *Mycobacterium marinum* (*Mm*)
21 infection, to study the effect of glucocorticoids. Our results show that the synthetic glucocorticoid
22 beclomethasone increases the bacterial burden and the dissemination of a systemic *Mm* infection.
23 The exacerbated *Mm* infection was associated with a decreased phagocytic activity of macrophages,
24 higher percentages of extracellular bacteria, and a reduced rate of infected cell death, whereas the
25 bactericidal capacity of the macrophages was not affected. The inhibited phagocytic capacity of
26 macrophages was associated with suppression of the transcription of genes involved in phagocytosis
27 in these cells. The decreased bacterial phagocytosis by macrophages was not specific for *Mm*, since it
28 was also observed upon infection with *Salmonella* Typhimurium. In conclusion, our results show that
29 glucocorticoids inhibit the phagocytic activity of macrophages, which may increase the severity of
30 bacterial infections like tuberculosis.

31 Introduction

32 Glucocorticoids (GCs) are a class of steroid hormones that are secreted upon stress. The main
33 endogenous GC in our body, cortisol, helps our bodies adapt to stressful situations and for this
34 purpose it regulates a wide variety of systems, like the immune, metabolic, reproductive,
35 cardiovascular and central nervous system. These effects are mediated by an intracellular receptor,
36 the glucocorticoid receptor (GR), which acts as a ligand-activated transcription factor. Synthetic GCs
37 are widely prescribed to treat various immune-related diseases due to their potent suppressive
38 effects on the immune system. However, prolonged therapy with these pleiotropic steroids evokes
39 severe side effects, such as osteoporosis and diabetes mellitus (Buckley and Humphrey, 2018; Suh
40 and Park, 2017). Importantly, the therapeutic immunosuppressive effect of GCs may lead to
41 infectious complications because of the compromised immune system (Caplan et al., 2017; Dixon et
42 al., 2011; Fardet et al., 2016). Similarly, after chronic stress an increased susceptibility to infectious
43 diseases has been observed, due to the high circulating levels of cortisol. In order to better
44 understand these complex effects of GCs, more research is required into how GCs influence the
45 susceptibility to infections and the course of infectious diseases.

46 Tuberculosis (TB) is the most prevalent bacterial infectious disease in the world, caused by the
47 pathogen *Mycobacterium tuberculosis* (*Mtb*). Despite the efforts made to reach the “End TB Strategy”
48 of the World Health Organization, *Mtb* still infects approximately one-quarter of the world's
49 population and caused an estimated 1.5 million deaths in 2018, which makes it one of the top 10
50 causes of death globally (Houben and Dodd, 2016; World Health Organization, 2019). The major
51 characteristic of *Mtb* infection is the formation of granulomas containing infected and non-infected
52 immune cells (Furin et al., 2019). Most *Mtb*-infected people develop a latent, noncontagious
53 infection and do not show any symptoms, with the bacteria remaining inactive, while contained
54 within granulomas (Drain et al., 2018; Lin and Flynn, 2010). About 5-10% of the carriers develop a
55 clinically active TB disease associated with a loss of granuloma integrity (Lin and Flynn, 2010; Parikka
56 et al., 2012). Among those TB patients, the majority manifest a lung infection and around 20% shows
57 infection in other organs like the central nervous system, pleura, urogenital tracts, bones and joints,
58 and lymph nodes (Kulchavenya, 2014). Antibiotics are currently the mainstay for TB treatment, but
59 since antibiotic resistance is rising and an effective vaccine against latent or reactivated TB is still
60 lacking, alternative therapies to control TB are needed (Hawn et al., 2013).

61 GCs are known to modulate the pathogenesis of TB, but their effects are highly complicated. The use
62 of GCs is considered as a risk factor for TB. Patients who are being treated with GCs have an
63 approximately 5-fold increased risk for developing new TB (Jick et al., 2006), and treatment with a

64 moderate or high dose of GCs is associated with an increased risk of activation of latent TB
65 (Bovornkitti et al., 1960; Kim et al., 1998; Schatz et al., 1976). Consequently, a tuberculin skin test
66 (TST) for screening latent TB is recommended before starting GC therapy (Jick et al., 2006). Moreover,
67 chronic stress which is associated with increased circulating levels of the endogenous GC cortisol, has
68 been shown to be associated with a higher incidence of TB (Lerner, 1996).

69 Despite the generally detrimental effects of GCs on TB susceptibility and progression, certain types of
70 TB patients are treated with GCs. Chronic TB patients may require GCs for treatment of other
71 disorders, and it has been shown that adjunctive GC therapy may have beneficial effects.
72 Traditionally, adjunctive GC with standard anti-TB therapy has been used for prevention of
73 inflammatory complications in patients with tuberculous meningitis, pericarditis, and pleurisy (Alzeer
74 and FitzGerald, 1993; Evans, 2008; Kadhiravan and Deepanjali, 2010; Singh and Tiwari, 2017). It has
75 been reported that adjunctive GC therapy could improve the probability of survival in tuberculous
76 meningitis and pericarditis (Strang et al., 2004; Thwaites et al., 2004; Torok et al., 2011; Wiysonge et
77 al., 2017). In case of pulmonary TB, the most common form of TB, adjunctive GC therapy is
78 recommended in advanced tuberculosis since broad and significant clinical benefits have been
79 demonstrated (Muthuswamy et al., 1995; Smego and Ahmed, 2003).

80 Although GCs are being used for adjunctive therapy, the beneficial effects of GC treatment are still
81 under debate. For tuberculous pleurisy TB, the efficacy of GCs is still controversial and for meningitis
82 and pericarditis, information on the GC effects is still incomplete (Prasad et al., 2016; Ryan et al.,
83 2017; Singh and Tiwari, 2017; Wiysonge et al., 2017). A review regarding clinical trials for pulmonary
84 TB showed that, although adjunctive GC therapy appears to have short-term benefits, it is not
85 maintained in the long-term (Critchley et al., 2014). An explanation for the complexity of the effects
86 of GC therapy in TB has been offered by Tobin et al. (2012). They showed that patients suffer from TB
87 as a result of either a failed or an excessive immune response to the mycobacterial infection, and
88 that only the subset of TB meningitis patients with an excessive response, showing a
89 hyperinflammatory phenotype (in their study as a result of a polymorphism in the *LTA4H* gene),
90 benefited from adjunctive GC therapy. It was suggested that GCs may also be beneficial for similar
91 subgroups of patients suffering from other forms of TB (Tobin et al., 2012).

92 The complex interplay between GC actions and TB underscores the need for a better understanding
93 of the effects of GCs on mycobacterial infection. In the present study we have studied these effects
94 using *Mycobacterium marinum* (*Mm*) infection in zebrafish as a model system. *Mm* is a species
95 closely related to *Mtb* that can infect zebrafish and other cold-blooded animals naturally, causing a
96 TB-like disease (Tobin and Ramakrishnan, 2008). Infection of zebrafish larvae with *Mm* provides an

97 animal model system that mimics hallmark aspects of *Mtb* infection in humans and is widely used for
98 research into mechanisms underlying the course of this disease (Cronan and Tobin, 2014; Meijer,
99 2016; Ramakrishnan, 2013). Like *Mtb*, *Mm* is able to survive and replicate within macrophages and,
100 in later stages of infection, induces the formation of granulomas (Davis et al., 2002). The
101 transparency of zebrafish at early life stages makes it possible to perform non-invasive long-term live
102 imaging, which has been used to reveal the earliest stages of granuloma formation (Davis and
103 Ramakrishnan, 2009). In addition, the availability of different transgenic and mutant zebrafish lines
104 and the efficient application of molecular techniques allow us to exploit this zebrafish *Mm* infection
105 model optimally to study both the host factors and bacterial factors involved in mycobacterial
106 infection processes (Meijer, 2016; Tobin and Ramakrishnan, 2008; van Leeuwen et al., 2015). For
107 example, zebrafish studies revealed that infected macrophages can detach from a granuloma and
108 facilitate dissemination to new locations (Davis and Ramakrishnan, 2009). Moreover, the study of an
109 *lta4h* mutant zebrafish line showed that the polymorphism in the *LTA4H* gene is associated with the
110 susceptibility to mycobacterial diseases and the response to adjunctive GC therapy in human,
111 representing a prime example of translational research (Tobin et al., 2012; Tobin et al., 2010).

112 The zebrafish has proven to be a suitable model for studying the effects of GCs, since the GC
113 signaling pathway is very well conserved between zebrafish and humans. Both humans and zebrafish
114 have a single gene encoding the GR, and the organization of these genes is highly similar (Alsop and
115 Vijayan, 2008; Schaaf et al., 2009; Stolte et al., 2006). Both the human and the zebrafish gene
116 encodes two splice variants, the α -isoform, the canonical receptor, and the β -isoform, which has no
117 transcriptional activity (Schaaf et al., 2009). The DNA binding domain (DBD) and ligand binding
118 domain (LBD) of the canonical α -isoform of the human and zebrafish GR share similarities of 98.4%
119 and 86.5% respectively (Schaaf et al., 2009). The zebrafish GR α -isoform, hereafter referred to as Gr,
120 mediates GC effects that have traditionally been observed in humans and other mammals as well,
121 like the effects on metabolism (Chatzopoulou et al., 2015) and the suppression of the immune
122 system (Chatzopoulou et al., 2016). This makes the zebrafish an ideal model to study the mechanisms
123 of GC action *in vivo* (Facchinello et al., 2017; Faught and Vijayan, 2019). In a recent study, we have
124 demonstrated that GC treatment inhibits the activation of the immune system in zebrafish larvae
125 upon wounding (Xie et al., 2019). The migration of the neutrophils and the differentiation of
126 macrophages was attenuated upon treatment with the synthetic GC.

127 In the present study, to investigate the functional consequences of the previously observed GC
128 effects on immune cells, we have investigated how GCs modulate the course of an *Mm* infection in
129 zebrafish larvae. We demonstrate that beclomethasone increases the level of *Mm* infection and
130 tissue dissemination. This increased *Mm* infection can be explained by an inhibition of the phagocytic

131 activity of macrophages by beclomethasone, which did not affect the microbicidal capacity of these
132 cells. The inhibitory effect of beclomethasone on phagocytosis, which most likely results from Gr
133 interfering with the transcription of genes required for phagocytosis, results in a higher percentage
134 of extracellular bacteria, which eventually leads to an exacerbation of the *Mm* infection.

135

136 **Results**

137 **Beclomethasone increases mycobacterial infection through Glucocorticoid receptor (Gr)**
138 **activation**

139 To study the effect of GC treatment on *Mm* infection in zebrafish, we pretreated zebrafish embryos
140 with beclomethasone and infected them intravenously with fluorescently labelled *Mm*. At 4 days
141 post infection (dpi), the bacterial burden was assessed by quantification of pixel intensities of
142 fluorescence microscopy images. We found that the bacterial burden increased by 2.3 fold when
143 embryos were treated with 25 μ M beclomethasone compared with the vehicle-treated group (Figure
144 1 A, C). Beclomethasone treatment at lower concentrations of 0.04, 0.2, 1 and 5 μ M did not affect
145 the bacterial burden. Therefore, a concentration of 25 μ M beclomethasone was used in subsequent
146 experiments. We have previously shown that this concentration effectively reduces wound-induced
147 leukocyte migration in zebrafish as well (Xie et al., 2019).

148 To demonstrate that the beclomethasone-induced increase in bacterial burden was not due to a
149 general toxicity of beclomethasone but mediated specifically by the Gr, we used the GR antagonist
150 RU-486. The results of these experiments showed that the beclomethasone-induced increase in
151 bacterial burden at 4 dpi was abolished when co-treatment with RU-486 was applied (Figure 1 B, D),
152 which indicates that the effect of beclomethasone requires activation of Gr. No significant difference
153 was observed when the RU-486-treated larvae were compared to the vehicle-treated group. In
154 conclusion, beclomethasone increases the level of *Mm* infection in zebrafish larvae and this effect is
155 mediated by Gr.

156 **Beclomethasone treatment leads to a higher infection and dissemination level without**
157 **influencing the microbicidal capacity of macrophages**

158 Subsequently, we analyzed the effect of beclomethasone on *Mm* infection in more detail. The total
159 bacterial burden (Figure 2 A), the number of bacterial clusters per individual (Figure 2 B) and the
160 average size of the bacterial clusters (Figure 2 C) were quantified at 1, 2, 3 and 4 dpi. The results

161 showed that the difference in bacterial burden between the beclomethasone-treated group and the
162 vehicle group was not significant at 1-3 dpi, but that a significant difference was observed at 4 dpi
163 (6186.1 ± 626.5 vs 2870.5 ± 235.0). However, a significant increase in the number of bacterial clusters
164 in the beclomethasone-treated group was already detected at 3 dpi (28.3 ± 1.9 vs 18.1 ± 1.5 in the
165 vehicle group) which was sustained at 4 dpi (64.2 ± 3.5 vs 35.4 ± 2.6). The size of the bacterial clusters
166 at 4 dpi was also increased in the beclomethasone-treated group compared to the cluster size in the
167 vehicle-treated group (741.6 ± 58.3 vs 498.3 ± 45.7). The increase in the number of bacterial clusters
168 indicates an increased dissemination of the infection due to beclomethasone treatment. We
169 confirmed this effect of beclomethasone on bacterial dissemination using hindbrain infection (Figure
170 2 D, E). Following *Mm* injection into the hindbrain ventricle, $66.1 \pm 2.0\%$ of embryos in the vehicle-
171 treated group showed disseminated infection in tissues of the head and tail at 24 hours post
172 infection (hpi), while a significantly higher number ($76.4 \pm 2.6\%$) showed this dissemination in the
173 beclomethasone-treated group.

174 To study whether the increased infection and dissemination was related to the microbicidal capacity
175 of macrophages, we injected *Mm Δerp* bacteria which are deficient for growth inside macrophages
176 (Clay et al., 2008). No significant difference was observed for the number of *Mm* clusters (Figure 3A)
177 and the percentage of *Mm* inside macrophage (Figure 3B) between the beclomethasone-treated
178 group and the vehicle-treated group. To assess the ability of macrophages to kill bacteria, we
179 quantitated the percentage of bacteria-containing macrophages that contained only 1-10 bacteria in
180 the tail region at 44 hpi (Sommer et al., 2020). There was no significant difference in this percentage
181 between the vehicle-treated group ($82.0 \pm 4.9\%$) and the beclomethasone-treated group ($81.6 \pm 5.0\%$)
182 (Figure 3C-E). Taken together, these findings indicate that beclomethasone treatment leads to a
183 higher overall *Mm* infection level and increased dissemination, and that these effects are not related
184 to an altered microbicidal capacity of macrophages.

185 **Beclomethasone activation of Gr inhibits macrophage phagocytic activity**

186 Since previous studies showed that increased *Mm* infection could be related to decreased phagocytic
187 activity of macrophages in zebrafish (Benard et al., 2014), we studied the effect of beclomethasone
188 on phagocytosis. We used the *Tg(mpeg1:mCherry-F)* line in which macrophages are fluorescently
189 labeled, and assessed phagocytic activity of macrophages by determining the percentage of *Mm* that
190 were internalized by macrophages in the yolk sac area (Benard et al., 2014) (Figure 4 A-C). In the
191 vehicle-treated group, the percentage of phagocytosed *Mm* was $17.4 \pm 3.5\%$ at 5 minutes post
192 infection (mpi) and gradually increased to $41.9 \pm 4.9\%$ and $52.8 \pm 5.2\%$ at 15 and 25 mpi respectively. At
193 each of these time points, a lower percentage of *Mm* were phagocytosed in the beclomethasone-

194 treated group ($4.6\pm1.6\%$ at 5 mpi, $25.7\pm4.7\%$ at 15 mpi and $34.0\pm5.2\%$ at 25 mpi). In addition, we
195 studied the involvement of Gr in the beclomethasone-induced inhibition of phagocytosis at 5 mpi, by
196 co-treatment with the GR antagonist RU-486 (Figure 4 D). We found that the decreased phagocytic
197 activity that was observed upon beclomethasone treatment was abolished when larvae were co-
198 treated with RU-486, indicating that the inhibition of phagocytosis by beclomethasone is mediated
199 by Gr.

200 Gr generally acts as a transcription factor, modulating the transcription rate of a wide variety of
201 genes. To study whether phagocytosis could be modulated by altering the process of protein
202 synthesis, we blocked *de novo* protein synthesis by treatment with cycloheximide (Figure 4 D). We
203 observed that the phagocytic activity of macrophages at 5 mpi was decreased by the cycloheximide
204 treatment ($3.4\pm1.0\%$ vs $11.1\pm1.8\%$ in the vehicle group). These data demonstrate that phagocytosis
205 depends on *de novo* protein synthesis, and suggest that modulating transcription could be the
206 mechanism underlying the inhibition of phagocytosis by Gr.

207 **Beclomethasone treatment results in fewer intracellular bacteria and limits infected cell
208 death**

209 To further analyze the possible mechanisms underlying the beclomethasone-induced increase in the
210 *Mm* infection level, we assessed the percentage of bacteria that are present inside and outside
211 macrophages in the caudal hematopoietic tissue (CHT) at 48 hpi using *Mm* infection in the
212 *Tg(mpeg1:GFP)* line. The results showed that beclomethasone treatment resulted in a decreased
213 percentage of intracellular bacteria ($23.8\pm3.0\%$) compared to the percentage in the vehicle-treated
214 group ($36.5\pm3.6\%$) (Figure 5 A, C). This result was in line with the observed decrease in phagocytosis
215 at earlier stages of infection. Finally, we used terminal deoxynucleotidyl transferase dUTP nick end
216 labelling (TUNEL) staining to detect cell death, and we performed this staining at 48 hpi (Zhang et al.,
217 2019). In the beclomethasone-treated group, the percentage of *Mm* that were colocalized with
218 TUNEL staining ($9.4\pm1.6\%$) was significantly lower compared to the percentage of the vehicle group
219 ($17.2\pm2.3\%$) (Figure 5 B, D). These data suggest that the observed inhibition of phagocytosis upon
220 beclomethasone treatment causes a decrease in the percentage of intracellular bacteria, which
221 underlies the lower numbers of macrophages undergoing cell death as a result of the *Mm* infection.

222 **Beclomethasone inhibits phagocytosis-related gene expression in macrophages**

223 To unravel the molecular mechanisms underlying the beclomethasone-induced inhibition of the
224 phagocytic activity of macrophages, we performed qPCR analysis on FACS-sorted macrophages
225 derived from 28 hpf larvae after 2 h of beclomethasone treatment. To determine the phenotype of

226 the sorted macrophages, the expression of a classic pro-inflammatory gene, *tnfa*, was measured
227 (Martinez and Gordon, 2014; Nguyen-Chi et al., 2015). The levels of *tnfa* expression were significantly
228 lower after beclomethasone treatment (Figure 6 A), in agreement with previously reported
229 transcriptome analysis (Xie et al., 2019). In addition, we measured the expression levels of seven
230 phagocytosis-related genes, *sparcl1*, *uchl1*, *ube2v1*, *marcksa*, *marcksb*, *bsg* and *tubb5* (Banerjee et al.,
231 2019; Carballo et al., 1999; Jeon et al., 2010) (Figure 6 B-H). The expression levels of four of these
232 genes, *sparcl1*, *uchl1*, *marcksa* and *marcksb*, were inhibited by beclomethasone treatment, while the
233 levels of the other three (*ube2v1*, *bsg* and *tubb5*) were not affected. These data suggest that
234 beclomethasone inhibits the phagocytic activity of macrophages by suppressing the transcription of
235 phagocytosis-related genes in these cells.

236 **Effect of Beclomethasone on the phagocytosis of *Salmonella* Typhimurium**

237 To study whether the beclomethasone-induced inhibitory effect on macrophage phagocytosis of *Mm*
238 can be generalized to other bacterial infections, we analyzed the effect of beclomethasone on
239 infection with *Salmonella* Typhimurium, which is also an intracellular pathogen, but belongs to the
240 gram-negative class. We quantified the percentages of bacteria phagocytosed by macrophages at
241 different time points after infection in the *Tg(mpeg1:GFP)* fish line (Figure 7). In the vehicle group,
242 the percentage of phagocytosed *Salmonella* Typhimurium increased from 5.7±0.7% at 10 mpi to
243 9.0±1.2% at 30 mpi and 17.9±1.7% at 60 mpi, and these percentages were significantly lower in the
244 beclomethasone-treated group at all time points (3.1±0.5% at 10 mpi, 6.5±1.0% at 30 mpi and
245 10.0±1.4% at 60 mpi). These data demonstrate that the inhibitory effect of beclomethasone on the
246 phagocytic activity of macrophages is not specific for *Mm*, but can also be observed for a distantly
247 related *Salmonella* species.

248

249 **Discussion**

250 Synthetic GCs are widely prescribed to treat various immune-related diseases, but their clinical use is
251 limited by the severe side effects evoked by prolonged therapy, including a higher susceptibility to TB
252 (Caplan et al., 2017; Jick et al., 2006). In order to gain more insight into the mechanism underlying
253 this GC effect, we used the zebrafish *Mm* infection model, which mimics human TB, and studied the
254 effect of GC treatment on the development of the infection. We showed that GC treatment
255 increased the level of *Mm* infection, which was reflected in the overall bacterial burden, the size and
256 number of bacterial clusters and the level of dissemination. Since we found that GC treatment

257 inhibited the phagocytic activity but not the microbicidal capacity of macrophages, we propose that
258 the GC-induced increase in infection susceptibility is due to the inhibition on phagocytosis. Analysis
259 of the transcription level of phagocytosis-related genes in macrophages suggested that the inhibition
260 of phagocytic activity by GCs is mediated by Gr interfering with phagocytosis-related gene
261 transcription. As a result of the lower phagocytic activity of the macrophages, the percentage of
262 intracellular bacteria is decreased, which results in a lower level of cell death due to the *Mm*
263 infection and exacerbated growth of the extracellular bacterial fraction. Finally, we showed that GC
264 treatment not only limited phagocytosis of mycobacteria, but also of a *Salmonella* species, which
265 suggests that the decrease in phagocytic activity may also explain the increased susceptibility to
266 other bacterial infections that is commonly observed in patients receiving GC therapy (Caplan et al.,
267 2017; Dixon et al., 2011; Fardet et al., 2016).

268 Upon bacterial infections, macrophages are the first responders of the immune system. In humans,
269 *Mtb* generally infects lungs due to its air transmission properties and in the lungs it is taken up by
270 alveolar macrophages within the first few days. In later stages, *Mtb* replicates, translocates to
271 secondary loci and aggregates into granulomas with other attracted immune cells (Cambier et al.,
272 2014; Russell, 2011; Srivastava et al., 2014). Consistently, in the zebrafish model, *Mm* is
273 predominantly phagocytosed by macrophages within 30-60 min after intravenous infection in
274 embryos, leading to initial stages of granuloma formation in the next few days (Benard et al., 2014;
275 Davis et al., 2002). The phagocytosis activity and microbicidal capacity of macrophages have both
276 been shown to be important for dealing with *Mm* infection (Benard et al., 2014; Clay et al., 2007).
277 Interestingly, in our study we found that the microbicidal capacity of macrophages was not affected
278 by GC treatment, which suggests that the inhibition of macrophage phagocytosis is a specific effect
279 of GCs targeted at the uptake of pathogens rather than a global suppression of anti-microbial
280 processes in macrophages.

281 Our study in the zebrafish model provides *in vivo* evidence for GC interference with macrophage
282 phagocytosis that confirms results from various other studies. In line with our results, it has
283 previously been shown that GCs decrease the phagocytosis of several *Escherichia coli* strains by
284 human monocyte-derived (THP-1) macrophages and by murine bone marrow-derived macrophages
285 (BMDMs) (Olivares-Morales et al., 2018). Similarly to our results, in this study the reduced
286 phagocytosis activity was accompanied by a decreased expression of genes involved in phagosome
287 formation including *MARCKS* and pro-inflammatory genes like *TNF* (Olivares-Morales et al., 2018). In
288 earlier studies, decreased macrophage phagocytosis of carbon particles was observed *in vivo*, in GC-
289 treated rats and rheumatoid arthritis patients (Jessop et al., 1973; Vernon-Roberts et al., 1973).

290 In contrast to our results on phagocytosis of mycobacteria, in other studies GC treatment has been
291 shown to enhance the phagocytosis activity of macrophages. Upon GC exposure, increased
292 phagocytosis of human monocyte-derived macrophages was observed for *Haemophilus influenzae*
293 and *Streptococcus pneumoniae* (Taylor et al., 2010), and *Staphylococcus aureus* (van der Goes et al.,
294 2000). This increased phagocytic activity would be in line with the well-established GC-induced
295 enhancement of the phagocytosis of apoptotic neutrophils, which has been observed in,
296 differentiated THP-1 macrophages, through stimulation of a protein S/Mer tyrosine kinase
297 dependent pathway (Liu et al., 1999; McColl et al., 2009; Zahuczky et al., 2011), and in mouse
298 alveolar macrophages (McCubrey et al., 2012). This effect is considered to play an important role in
299 GCs actively promoting the resolution of inflammation and reflects the GC-enhanced differentiation
300 of macrophages to an anti-inflammatory phenotype (Busillo and Cidlowski, 2013; Ehrchen et al.,
301 2019). Interestingly, GC treatment does not enhance the phagocytosis capacity in differentiated THP-
302 1 macrophages of latex beads or apoptotic cells (Zahuczky et al., 2011). Most likely, the effects of GCs
303 on the phagocytic activity of macrophages are highly dependent on the differentiation status of the
304 cells, the particles they encounter and the tissue environment.

305 Our study revealed an inhibitory effect of GCs on four phagocytosis-related genes in FACS-sorted
306 macrophages: *sparcl-1*, *uchl-1*, *marcksa* and *marcksb*. Among those genes, the human and mouse
307 homologs of *sparcl-1* and *uchl-1* were reported to have a phagocytosis-promoting activity (Banerjee
308 et al., 2019; Jeon et al., 2010). In human THP-1-derived macrophages, MARCKS plays a role in
309 cytoskeletal remodeling and phagosome formation, and in line with our study the MARCKS gene
310 expression was found to be inhibited by dexamethasone treatment (Carballo et al., 1999; Olivares-
311 Morales et al., 2018). Together with our observation that phagocytosis is dependent on *de novo*
312 protein synthesis, these results support the idea that GC treatment inhibits the phagocytosis activity
313 of macrophages through interfering with transcription of genes that stimulate the phagocytic activity.

314 After internalization by macrophages, *Mm* are exposed to a bactericidal environment (Lesley and
315 Ramakrishnan, 2008). Some bacteria may be killed by macrophages, while others may proliferate
316 mediated by virulence determinants like Erp and RD1 (Clay et al., 2008; Lesley and Ramakrishnan,
317 2008; Lewis et al., 2003). When the macrophages are incapable of containing the bacteria, they
318 undergo cell death leading to recruitment of more macrophages (Davis and Ramakrishnan, 2009). In
319 our study, GC treatment led to a lower percentage of intracellular *Mm* at later stages, consistent with
320 the decreased phagocytosis at early time points, and consequently less *Mm*-related cell death. The
321 GC treatment may also directly affect cell death, since in a recent study it was demonstrated that GCs
322 inhibit necrosis of various *Mtb* infected mouse and human cell types by activating MKP-1, which
323 suppresses a pathway involving p38 MAPK activation ultimately leading to a loss of mitochondrial

324 integrity (Gräb et al., 2019). The increased numbers of extracellular bacteria could traverse
325 endothelial barriers directly and grow more rapidly in a less restrictive environment outside
326 macrophages, which may explain our observation of a higher bacterial burden induced by GC
327 treatment.

328 Based on our results, it may seem surprising that adjunctive GC therapy is often beneficial to TB
329 patients, and even increases survival among tuberculous meningitis and pericarditis patients (Strang
330 et al., 2004; Thwaites et al., 2004; Wiysonge et al., 2017). However, many of these observed
331 beneficial effects are either minor or under debate. This may be due to GC therapy benefiting only a
332 subset of patients whose disease has mainly progressed as a result of an excessive inflammatory
333 response (which can be controlled with GC therapy), rather than a failed reaction to the infection,
334 which was demonstrated for GC-treated TB meningitis patients with specific polymorphisms in the
335 *LTA4H* gene (Tobin et al., 2012). We therefore suggest that in a subset of patients at later stages of
336 infection, the anti-inflammatory effects of a GC treatment may outweigh a possible inhibitory effect
337 on the phagocytic activity of the macrophages. Further research using the zebrafish model may shed
338 light on a possible interplay between these effects, since the *Mm* infection model has been shown to
339 have excellent translational value for human TB, including the effects of GC treatment (Tobin 2010,
340 Tobin 2012).

341 In conclusion, our *in vivo* study on the effect of GC treatment in the zebrafish *Mm* infection model
342 shows that GCs, through activation of Gr, inhibit the phagocytic activity of macrophages, which
343 results in more extracellular bacterial growth and a higher infection level. These results may explain
344 why clinically prolonged GC treatment is associated with an increased risk of TB and other bacterial
345 infections.

346

347 **Materials and methods**

348 **Zebrafish lines and maintenance**

349 Zebrafish were maintained and handled according to the guidelines from the Zebrafish Model
350 Organism Database (<http://zfin.org>) and in compliance with the directives of the local animal welfare
351 body of Leiden University. They were exposed to a 14 hours light and 10 hours dark cycle to maintain
352 circadian rhythmicity. Fertilization was performed by natural spawning at the beginning of the light
353 period. Eggs were collected and raised at 28°C in egg water (60 µg/ml Instant Ocean sea salts and
354 0.0025% methylene blue). The following fish lines were used: wild type strain AB TL, and the

355 transgenic lines *Tg(mpeg1:mCherry-F^{umsF001})* (Bernut et al., 2014) and *Tg(mpeg1:eGFP^{gl22})* (Ellett et al.,
356 2011).

357 **Bacterial culture and infection through intravenous injections**

358 Bacteria used for this study were *Mycobacterium marinum*, strain M, constitutively fluorescently
359 labelled with Wasabi or mCrimson (Ramakrishnan and Falkow, 1994; Takaki et al., 2013), *Mm* mutant
360 Δ erp labelled with Wasabi (Cosma et al., 2006), and *Salmonella enterica* serovar Typhimurium (*S.*
361 Typhimurium) wild type (wt) strain SL1344 labelled with mCherry (Burton et al., 2014; Hoiseth and
362 Stocker, 1981). The *Mm* strain M and *S. Typhimurium* wt strain were cultured at 28°C and 37°C
363 respectively and the bacterial suspensions were prepared with phosphate buffered saline (PBS) with
364 2% (w/v) polyvinylpyrrolidone-40 (PVP40, Sigma-Aldrich), as previously described (Benard et al.,
365 2012). The suspension of *Mm* Δ erp-Wasabi was prepared directly from -80°C frozen aliquots.

366 After anesthesia with 0.02% aminobenzoic acid ethyl ester (tricaine, Sigma-Aldrich), 28 hours post
367 fertilization (hpf) embryos were injected with *Mm* or *S. Typhimurium* into the blood island (or
368 hindbrain if specified) under a Leica M165C stereomicroscope, as previously described (Benard et al.,
369 2012). The injection dose was 200 CFU for *Mm* and 50 CFU for *S. Typhimurium*.

370 **Chemical treatments and bacterial burden quantification**

371 The embryos were treated with 25 μ M (or different if specified) beclomethasone (Sigma-Aldrich) or
372 vehicle (0.05% dimethyl sulfoxide (DMSO)) in egg water from 2 hours before injection to the end of
373 an experiment. RU-486 (Sigma-Aldrich) was administered at a concentration of 5 μ M (0.02% DMSO),
374 and cycloheximide (Sigma-Aldrich) at 100 μ g/ml (0.04% DMSO). If the treatment lasted longer than 1
375 day, the medium was refreshed every day.

376 For bacterial burden quantification, the embryos from the vehicle- and beclomethasone-treated
377 groups were imaged alive using a Leica M205FA fluorescence stereomicroscope equipped with a
378 Leica DFC 345FX camera (Leica Microsystems). The images were analyzed using custom-designed
379 pixel quantification software (previously described by Benard et al. (2015)), and Image J (plugin
380 'Analyze Particles').

381 **Hindbrain infection and analysis of dissemination**

382 To assess the dissemination efficiency, the embryos were injected with 50 CFU *Mm* into the
383 hindbrain at 28 hpf. At 2 dpi, the embryos were imaged with a Leica M205FA fluorescence
384 stereomicroscope equipped with a Leica DFC 345FX camera. The embryos were classified into two

385 categories: with or without disseminated infection. An embryo was considered without disseminated
386 infection if all the bacteria were still contained in the hindbrain ventricle and considered with
387 dissemination if bacteria were present in any other part of the embryo.

388 **Analysis of microbicidal activity**

389 After infection at 28 hpf with *Mm Δerp*-Wasabi, *Tg(mpeg1:mCherry-F)* embryos were fixed at 44 hpi
390 with 4% paraformaldehyde (PFA, Sigma-Aldrich) and imaged using a Leica TCS SP8 confocal
391 microscope with 40X objective (NA 1.3). All macrophages that contained *Mm Δerp*-Wasabi in the tail
392 region were analyzed. The level of infection inside macrophages was classified into two categories
393 based on the number of bacteria: 1-10 bacteria or >10 bacteria, following established protocols (Clay
394 et al., 2008; Sommer et al., 2020).

395 **Analysis of phagocytic activity**

396 After infection at 28 hpf with *Mm*-Wasabi or *S. Typhimurium*-mCherry, *Tg(mpeg1:mCherry-F)* or
397 *Tg(mpeg1:GFP)* embryos were fixed with 4% PFA at different time points and imaged using a Leica
398 TCS SP8 confocal microscope with 20X objective (NA 0.75). The yolk sac area was selected as the
399 quantification area (Figure 4A). The number of fluorescently labelled *Mm* or *S. Typhimurium* in this
400 area, and those present inside a macrophage, were counted in a manual and blinded way.

401 **TUNEL assay**

402 After infection at 28 hpf, *Tg(mpeg1:mCherry-F)* embryos were fixed with 4% PFA at 48 hpi and
403 stained using terminal deoxynucleotidyl transferase dUTP nick end labelling (TUNEL) with the In Situ
404 Cell Death Detection Kit, TMR red (Sigma-Aldrich), as previously described by Zhang et al. (2019). For
405 this TUNEL staining, the embryos were first dehydrated and then rehydrated gradually with
406 methanol in PBS, and permeabilized with 10 µg/ml Proteinase K (Roche). The embryos were
407 subsequently fixed with 4% PFA for another 20 min and stained with reagent mixture overnight at
408 37°C. After the reaction was stopped by washing with PBS containing 0.05% Tween-20 (PBST), the
409 CHT region of the embryos was imaged using a Leica TCS SP8 confocal microscope with 40X objective
410 (NA 1.3). The total number of fluorescently labelled *Mm* clusters and the number of these clusters
411 overlapping with TUNEL staining were counted in a manual and blinded way.

412 **Fluorescence-Activated Cell Sorting (FACS) of macrophages**

413 Macrophages were sorted from *Tg(mpeg1:mCherry-F)* embryos as previously described (Rougeot et
414 al., 2014; Zakrzewska et al., 2010). Dissociation was performed with 150-200 embryos for each

415 sample after 2 hours beclomethasone or vehicle treatment (started at 28 hpf) using Liberase TL
416 (Roche) and stopped by adding Fetal Calf Serum (FCS) to a final concentration of 10%. Isolated cells
417 were resuspended in Dulbecco's PBS (DPBS), and filtered through a 40 µm cell strainer. Actinomycin
418 D (Sigma-Aldrich) was added (final concentration of 1 µg/ml) to each step to inhibit transcription.
419 Macrophages were sorted based on their red fluorescent signal using a FACSAria III cell sorter (BD
420 Biosciences). The sorted cells were collected in QIAzol lysis reagent (Qiagen) for RNA isolation.

421 **RNA isolation, cDNA synthesis and quantitative PCR (qPCR) analysis**

422 RNA isolation from FACS-sorted cells was performed using the miRNeasy mini kit (Qiagen), according
423 to the manufacturer's instructions. Extracted total RNA was reverse-transcribed using the iScript™
424 cDNA Synthesis Kit (Bio-Rad). QPCR was performed on a MyiQ Single-Color Real-Time PCR Detection
425 System (Bio-Rad) using iTaq™ Universal SYBR® Green Supermix (Bio-Rad). The sequences of the
426 primers used are provided in Supplementary Table 1. Cycling conditions were pre-denaturation for 3
427 min at 95°C, followed by 40 cycles of denaturation for 15 s at 95°C, annealing for 30 s at 60°C, and
428 elongation for 30 s at 72°C. Fluorescent signals were measured at the end of each cycle. Cycle
429 threshold values (Ct values, i.e. the cycle numbers at which a threshold value of the fluorescence
430 intensity was reached) were determined for each sample. To determine the gene regulation due to
431 beclomethasone treatment in each experiment, the average Ct value of the beclomethasone treated
432 samples was subtracted from the average Ct value of the vehicle-treated samples, and the fold
433 change of gene expression was calculated, which was subsequently adjusted to the expression levels
434 of a reference gene (*peptidylprolyl isomerase Ab (ppiab)*).

435 **Statistical analysis**

436 Statistical analysis was performed using GraphPad Prism by one-way ANOVA with Bonferroni's post
437 hoc test (Figure 1A) or two-way ANOVA with Tukey's post hoc test (Figure 1B, Figure 2 A-C) or two-
438 tailed t-test (Figure 2D, Figure 3, 5, 6) or using R Statistical Software by fitting data to a beta inflated
439 regression (from 'gamlss' package) (Stasinopoulos and Rigby, 2007) with Tukey's post hoc test (Figure
440 4, 7).

441

442 **Acknowledgements**

443 We thank Frida Sommer for her advice on *Mm Δerp* assays, Ralf Boland, Salomé Munoz Sanchez, Dr.
444 Michiel van der Vaart and Aleksandra Fesliyska for their assistance with bacterial infections, Dr. Rui
445 Zhang and Dr. Monica Varela Alvarez for their suggestions concerning TUNEL assays and Patrick van

446 Hage for his help with the statistical analysis. We thank the fish facility team, in particular Ulrike
447 Nehrdich, Ruth van Koppen, Karen Bosma and Guus van der Velden for zebrafish maintenance. We
448 thank Dr. Georges Lutfalla and Dr. Graham Lieschke for providing transgenic zebrafish lines.

449

450 **Competing interests**

451 No competing interests declared.

452

453 **Funding**

454 Yufei Xie was funded by a grant from the China Scholarship Council (CSC).

455 **References**

456 **Alsop, D. and Vijayan, M. M.** (2008). Development of the corticosteroid stress axis and
457 receptor expression in zebrafish. *Am J Physiol Regul Integr Comp Physiol* **294**, R711-9.

458 **Alzeer, A. H. and FitzGerald, J. M.** (1993). Corticosteroids and tuberculosis: risks and use as
459 adjunct therapy. *Tuber Lung Dis* **74**, 6-11.

460 **Banerjee, H., Krauss, C., Worthington, M., Banerjee, N., Walker, R. S., Hodges, S., Chen, L.,**
461 **Rawat, K., Dasgupta, S., Ghosh, S. et al.** (2019). Differential expression of efferocytosis and
462 phagocytosis associated genes in tumor associated macrophages exposed to African American
463 patient derived prostate cancer microenvironment. *J Solid Tumors* **9**, 22-27.

464 **Benard, E. L., Roobol, S. J., Spaink, H. P. and Meijer, A. H.** (2014). Phagocytosis of
465 mycobacteria by zebrafish macrophages is dependent on the scavenger receptor Marco, a key
466 control factor of pro-inflammatory signalling. *Dev Comp Immunol* **47**, 223-33.

467 **Benard, E. L., van der Sar, A. M., Ellett, F., Lieschke, G. J., Spaink, H. P. and Meijer, A. H.**
468 (2012). Infection of zebrafish embryos with intracellular bacterial pathogens. *J Vis Exp.*

469 **Bernut, A., Herrmann, J.-L., Kissa, K., Dubremetz, J.-F., Gaillard, J.-L., Lutfalla, G. and Kremer,**
470 **L.** (2014). Mycobacterium abscessus cording prevents phagocytosis and promotes abscess formation.
471 *Proceedings of the National Academy of Sciences* **111**, E943-E952.

472 **Bovornkitti, S., Kangsadal, P., Sathirapat, P. and Oonsombatti, P.** (1960). Reversion and
473 Reconversion Rate of Tuberculin Skin Reactions in Correlation with the Use of
474 Prednisone¹. *Diseases of the Chest* **38**, 51-55.

475 **Buckley, L. and Humphrey, M. B.** (2018). Glucocorticoid-Induced Osteoporosis. *N Engl J Med*
476 **379**, 2547-2556.

477 **Burton, N. A., Schürmann, N., Casse, O., Steeb, A. K., Claudi, B., Zankl, J., Schmidt, A. and**
478 **Bumann, D.** (2014). Disparate impact of oxidative host defenses determines the fate of *Salmonella*
479 during systemic infection in mice. *Cell Host & Microbe* **15**, 72-83.

480 **Busillo, J. M. and Cidlowski, J. A.** (2013). The five Rs of glucocorticoid action during
481 inflammation: ready, reinforce, repress, resolve, and restore. *Trends Endocrinol Metab* **24**, 109-19.

482 **Cambier, C. J., Falkow, S. and Ramakrishnan, L.** (2014). Host evasion and exploitation
483 schemes of *Mycobacterium tuberculosis*. *Cell* **159**, 1497-509.

484 **Caplan, A., Fett, N., Rosenbach, M., Werth, V. P. and Micheletti, R. G.** (2017). Prevention
485 and management of glucocorticoid-induced side effects: A comprehensive review: A review of
486 glucocorticoid pharmacology and bone health. *J Am Acad Dermatol* **76**, 1-9.

487 **Carballo, E., Pitterle, D. M., Stumpo, D. J., Sperling, R. T. and Blackshear, P. J.** (1999).

488 Phagocytic and macropinocytic activity in MARCKS-deficient macrophages and fibroblasts. *American*
489 *Journal of Physiology-Cell Physiology* **277**, C163-C173.

490 **Chatzopoulou, A., Heijmans, J. P., Burgerhout, E., Oskam, N., Spaink, H. P., Meijer, A. H. and**
491 **Schaaf, M. J.** (2016). Glucocorticoid-induced attenuation of the inflammatory response in zebrafish.
492 *Endocrinology* **157**, 2772-2784.

493 **Chatzopoulou, A., Roy, U., Meijer, A. H., Alia, A., Spaink, H. P. and Schaaf, M. J.** (2015).

494 Transcriptional and metabolic effects of glucocorticoid receptor α and β signaling in zebrafish.
495 *Endocrinology* **156**, 1757-1769.

496 **Clay, H., Davis, J. M., Beery, D., Huttenlocher, A., Lyons, S. E. and Ramakrishnan, L.** (2007).

497 Dichotomous role of the macrophage in early *Mycobacterium marinum* infection of the zebrafish.
498 *Cell Host Microbe* **2**, 29-39.

499 **Clay, H., Volkman, H. E. and Ramakrishnan, L.** (2008). Tumor necrosis factor signaling
500 mediates resistance to mycobacteria by inhibiting bacterial growth and macrophage death. *Immunity*
501 **29**, 283-94.

502 **Cosma, C. L., Klein, K., Kim, R., Beery, D. and Ramakrishnan, L.** (2006). *Mycobacterium*
503 *marinum* Erp is a virulence determinant required for cell wall integrity and intracellular survival.
504 *Infection and immunity* **74**, 3125-3133.

505 **Critchley, J. A., Orton, L. C. and Pearson, F.** (2014). Adjunctive steroid therapy for managing
506 pulmonary tuberculosis. *Cochrane Database Syst Rev*, Cd011370.

507 **Cronan, M. R. and Tobin, D. M.** (2014). Fit for consumption: zebrafish as a model for
508 tuberculosis. *Disease models & mechanisms* **7**, 777-784.

509 **Davis, J. M., Clay, H., Lewis, J. L., Ghori, N., Herbomel, P. and Ramakrishnan, L.** (2002). Real-
510 Time Visualization of *Mycobacterium*-Macrophage Interactions Leading to Initiation of Granuloma
511 Formation in Zebrafish Embryos. *Immunity* **17**, 693-702.

512 **Davis, J. M. and Ramakrishnan, L.** (2009). The Role of the Granuloma in Expansion and
513 Dissemination of Early Tuberculous Infection. *Cell* **136**, 37-49.

514 **Dixon, W., Kezouh, A., Bernatsky, S. and Suissa, S.** (2011). The influence of systemic
515 glucocorticoid therapy upon the risk of non-serious infection in older patients with rheumatoid
516 arthritis: a nested case-control study. *Annals of the rheumatic diseases* **70**, 956-960.

517 **Drain, P. K., Bajema, K. L., Dowdy, D., Dheda, K., Naidoo, K., Schumacher, S. G., Ma, S.,**
518 **Meermeier, E., Lewinsohn, D. M. and Sherman, D. R.** (2018). Incipient and Subclinical Tuberculosis: a
519 Clinical Review of Early Stages and Progression of Infection. *Clin Microbiol Rev* **31**.

520 **Ehrchen, J. M., Roth, J. and Barczyk-Kahlert, K.** (2019). More Than Suppression:
521 Glucocorticoid Action on Monocytes and Macrophages. *Front Immunol* **10**, 2028.

522 **Ellett, F., Pase, L., Hayman, J. W., Andrianopoulos, A. and Lieschke, G. J.** (2011). mpeg1
523 promoter transgenes direct macrophage-lineage expression in zebrafish. *Blood* **117**, e49-e56.

524 **Evans, D. J.** (2008). The use of adjunctive corticosteroids in the treatment of pericardial,
525 pleural and meningeal tuberculosis: Do they improve outcome? *Respiratory Medicine* **102**, 793-800.

526 **Facchinello, N., Skobo, T., Meneghetti, G., Colletti, E., Dinarello, A., Tiso, N., Costa, R.,**
527 **Gioacchini, G., Carnevali, O. and Argenton, F.** (2017). nr3c1 null mutant zebrafish are viable and
528 reveal DNA-binding-independent activities of the glucocorticoid receptor. *Scientific reports* **7**, 1-13.

529 **Fardet, L., Petersen, I. and Nazareth, I.** (2016). Common Infections in Patients Prescribed
530 Systemic Glucocorticoids in Primary Care: A Population-Based Cohort Study. *PLoS Med* **13**, e1002024.

531 **Faught, E. and Vijayan, M. M.** (2019). Loss of the glucocorticoid receptor in zebrafish
532 improves muscle glucose availability and increases growth. *Am J Physiol Endocrinol Metab* **316**,
533 E1093-e1104.

534 **Furin, J., Cox, H. and Pai, M.** (2019). Tuberculosis. *The Lancet* **393**, 1642-1656.

535 **Gräb, J., Suárez, I., van Gumpel, E., Winter, S., Schreiber, F., Esser, A., Hölscher, C., Fritsch,**
536 **M., Herb, M. and Schramm, M.** (2019). Corticosteroids inhibit *Mycobacterium tuberculosis*-induced
537 necrotic host cell death by abrogating mitochondrial membrane permeability transition. *Nature*
538 *communications* **10**, 1-14.

539 **Hawn, T. R., Matheson, A. I., Maley, S. N. and Vandal, O.** (2013). Host-directed therapeutics
540 for tuberculosis: can we harness the host? *Microbiol. Mol. Biol. Rev.* **77**, 608-627.

541 **Hoiseth, S. K. and Stocker, B.** (1981). Aromatic-dependent *Salmonella typhimurium* are non-
542 virulent and effective as live vaccines. *Nature* **291**, 238-239.

543 **Houben, R. M. and Dodd, P. J.** (2016). The global burden of latent tuberculosis infection: a
544 re-estimation using mathematical modelling. *PLoS Med* **13**, e1002152.

545 **Jeon, H., Go, Y., Seo, M., Lee, W. H. and Suk, K.** (2010). Functional selection of phagocytosis-
546 promoting genes: cell sorting-based selection. *J Biomol Screen* **15**, 949-55.

547 **Jessop, J., Vernon-Roberts, B. and Harris, J.** (1973). Effects of gold salts and prednisolone on
548 inflammatory cells. I. Phagocytic activity of macrophages and polymorphs in inflammatory exudates
549 studied by a "skin-window" technique in rheumatoid and control patients. *Annals of the rheumatic*
550 *diseases* **32**, 294.

551 **Jick, S. S., Lieberman, E. S., Rahman, M. U. and Choi, H. K.** (2006). Glucocorticoid use, other
552 associated factors, and the risk of tuberculosis. *Arthritis Rheum* **55**, 19-26.

553 **Kadhiravan, T. and Deepanjali, S.** (2010). Role of corticosteroids in the treatment of
554 tuberculosis: an evidence-based update. *Indian J Chest Dis Allied Sci* **52**, 153-8.

555 **Kim, H., Yoo, C., Baek, H., Lee, E. B., Ahn, C., Han, J., Kim, S., Lee, J.-S., Choe, K. and Song, Y.-W.** (1998). *Mycobacterium tuberculosis* infection in a corticosteroid-treated rheumatic disease patient population. *Clinical and experimental rheumatology* **16**, 9-13.

558 **Kulchavanya, E.** (2014). Extrapulmonary tuberculosis: are statistical reports accurate? *Therapeutic Advances in Infectious Disease* **2**, 61-70.

560 **Lerner, B. H.** (1996). Can stress cause disease? Revisiting the tuberculosis research of Thomas Holmes, 1949-1961. *Ann Intern Med* **124**, 673-80.

562 **Lesley, R. and Ramakrishnan, L.** (2008). Insights into early mycobacterial pathogenesis from the zebrafish. *Curr Opin Microbiol* **11**, 277-83.

564 **Lewis, K. N., Liao, R., Guinn, K. M., Hickey, M. J., Smith, S., Behr, M. A. and Sherman, D. R.** (2003). Deletion of RD1 from *Mycobacterium tuberculosis* mimics bacille Calmette-Guerin attenuation. *J Infect Dis* **187**, 117-23.

567 **Lin, P. L. and Flynn, J. L.** (2010). Understanding latent tuberculosis: a moving target. *The Journal of Immunology* **185**, 15-22.

569 **Liu, Y., Cousin, J. M., Hughes, J., Van Damme, J., Seckl, J. R., Haslett, C., Dransfield, I., Savill, J. and Rossi, A. G.** (1999). Glucocorticoids Promote Nonphlogistic Phagocytosis of Apoptotic Leukocytes. *The Journal of Immunology* **162**, 3639-3646.

572 **Martinez, F. O. and Gordon, S.** (2014). The M1 and M2 paradigm of macrophage activation: time for reassessment. *F1000Prime Rep* **6**, 13.

574 **McColl, A., Bournazos, S., Franz, S., Perretti, M., Morgan, B. P., Haslett, C. and Dransfield, I.** (2009). Glucocorticoids induce protein S-dependent phagocytosis of apoptotic neutrophils by human macrophages. *J Immunol* **183**, 2167-75.

577 **McCubrey, A. L., Sonstein, J., Ames, T. M., Freeman, C. M. and Curtis, J. L.** (2012). Glucocorticoids relieve collectin-driven suppression of apoptotic cell uptake in murine alveolar macrophages through downregulation of SIRP α . *The Journal of Immunology* **189**, 112-119.

580 **Meijer, A. H.** (2016). Protection and pathology in TB: learning from the zebrafish model. *Semin Immunopathol* **38**, 261-73.

582 **Muthuswamy, P., Hu, T.-C., Carasso, B., Antonio, M. and Dandamudi, N.** (1995). Prednisone as adjunctive therapy in the management of pulmonary tuberculosis: report of 12 cases and review of the literature. *CHEST* **107**, 1621-1630.

585 **Nguyen-Chi, M., Laplace-Builhe, B., Travnickova, J., Luz-Crawford, P., Tejedor, G., Phan, Q. T., Duroux-Richard, I., Levraud, J. P., Kissa, K., Lutfalla, G. et al.** (2015). Identification of polarized macrophage subsets in zebrafish. *Elife* **4**, e07288.

588 **Olivares-Morales, M. J., De La Fuente, M. K., Dubois-Camacho, K., Parada, D., Diaz-Jiménez, D., Torres-Riquelme, A., Xu, X., Chamorro-Veloso, N., Naves, R., Gonzalez, M.-J. et al.** (2018).

590 Glucocorticoids Impair Phagocytosis and Inflammatory Response Against Crohn's Disease-Associated
591 Adherent-Invasive *Escherichia coli*. *Frontiers in Immunology* **9**.

592 **Parikka, M., Hammaren, M. M., Harjula, S. K., Halfpenny, N. J., Oksanen, K. E., Lahtinen, M. J., Pajula, E. T., Iivanainen, A., Pesu, M. and Ramet, M.** (2012). *Mycobacterium marinum* causes a latent infection that can be reactivated by gamma irradiation in adult zebrafish. *PLoS Pathog* **8**, e1002944.

596 **Prasad, K., Singh, M. B. and Ryan, H.** (2016). Corticosteroids for managing tuberculous meningitis. *Cochrane Database of Systematic Reviews*.

598 **Ramakrishnan, L.** (2013). The zebrafish guide to tuberculosis immunity and treatment. *Cold Spring Harbor Symp Quant Biol* **78**, 179-92.

600 **Ramakrishnan, L. and Falkow, S.** (1994). *Mycobacterium marinum* persists in cultured mammalian cells in a temperature-restricted fashion. *Infection and immunity* **62**, 3222-3229.

602 **Rougeot, J., Zakrzewska, A., Kanwal, Z., Jansen, H. J., Spaink, H. P. and Meijer, A. H.** (2014). RNA sequencing of FACS-sorted immune cell populations from zebrafish infection models to identify cell specific responses to intracellular pathogens. *Methods Mol Biol* **1197**, 261-74.

605 **Russell, D. G.** (2011). Mycobacterium tuberculosis and the intimate discourse of a chronic infection. *Immunological reviews* **240**, 252-268.

607 **Ryan, H., Yoo, J. and Darsini, P.** (2017). Corticosteroids for tuberculous pleurisy. *Cochrane Database of Systematic Reviews*.

609 **Schaaf, M., Chatzopoulou, A. and Spaink, H.** (2009). The zebrafish as a model system for glucocorticoid receptor research. *Comparative Biochemistry and Physiology Part A: Molecular & Integrative Physiology* **153**, 75-82.

612 **Schatz, M., Patterson, R., Kloner, R. and Falk, J.** (1976). The prevalence of tuberculosis and positive tuberculin skin tests in a steroid-treated asthmatic population. *Ann Intern Med* **84**, 261-5.

614 **Singh, S. and Tiwari, K.** (2017). Use of corticosteroids in tuberculosis. *The Journal of Association of Chest Physicians* **5**, 70-75.

616 **Smego, R. A. and Ahmed, N.** (2003). A systematic review of the adjunctive use of systemic corticosteroids for pulmonary tuberculosis. *Int J Tuberc Lung Dis* **7**, 208-13.

618 **Sommer, F., Torracca, V., Kamel, S. M., Lombardi, A. and Meijer, A. H.** (2020). Frontline Science: Antagonism between regular and atypical Cxcr3 receptors regulates macrophage migration during infection and injury in zebrafish. *Journal of leukocyte biology* **107**, 185-203.

621 **Srivastava, S., Ernst, J. D. and Desvignes, L.** (2014). Beyond macrophages: the diversity of mononuclear cells in tuberculosis. *Immunol Rev* **262**, 179-92.

623 **Stasinopoulos, D. M. and Rigby, R. A.** (2007). Generalized additive models for location scale and shape (GAMLSS) in R. *Journal of Statistical Software* **23**, 1-46.

625 **Stolte, E. H., van Kemenade, B. L. V., Savelkoul, H. F. and Flik, G.** (2006). Evolution of
626 glucocorticoid receptors with different glucocorticoid sensitivity. *Journal of Endocrinology* **190**, 17-28.

627 **Strang, J. I., Nunn, A. J., Johnson, D. A., Casbard, A., Gibson, D. G. and Girling, D. J.** (2004).
628 Management of tuberculous constrictive pericarditis and tuberculous pericardial effusion in Transkei:
629 results at 10 years follow-up. *Qjm* **97**, 525-35.

630 **Suh, S. and Park, M. K.** (2017). Glucocorticoid-Induced Diabetes Mellitus: An Important but
631 Overlooked Problem. *Endocrinol Metab (Seoul)* **32**, 180-189.

632 **Takaki, K., Davis, J. M., Winglee, K. and Ramakrishnan, L.** (2013). Evaluation of the
633 pathogenesis and treatment of *Mycobacterium marinum* infection in zebrafish. *Nature protocols* **8**,
634 1114.

635 **Taylor, A., Finney-Hayward, T., Quint, J., Thomas, C., Tudhope, S., Wedzicha, J., Barnes, P.**
636 and **Donnelly, L.** (2010). Defective macrophage phagocytosis of bacteria in COPD. *European*
637 *Respiratory Journal* **35**, 1039-1047.

638 **Thwaites, G. E., Nguyen, D. B., Nguyen, H. D., Hoang, T. Q., Do, T. T., Nguyen, T. C., Nguyen,**
639 **Q. H., Nguyen, T. T., Nguyen, N. H., Nguyen, T. N.** et al. (2004). Dexamethasone for the treatment of
640 tuberculous meningitis in adolescents and adults. *N Engl J Med* **351**, 1741-51.

641 **Tobin, D. M. and Ramakrishnan, L.** (2008). Comparative pathogenesis of *Mycobacterium*
642 *marinum* and *Mycobacterium tuberculosis*. *Cellular microbiology* **10**, 1027-1039.

643 **Tobin, D. M., Roca, F. J., Oh, S. F., McFarland, R., Vickery, T. W., Ray, J. P., Ko, D. C., Zou, Y.,**
644 **Bang, N. D. and Chau, T. T.** (2012). Host genotype-specific therapies can optimize the inflammatory
645 response to mycobacterial infections. *Cell* **148**, 434-446.

646 **Tobin, D. M., Vary Jr, J. C., Ray, J. P., Walsh, G. S., Dunstan, S. J., Bang, N. D., Hagge, D. A.,**
647 **Khadge, S., King, M.-C. and Hawn, T. R.** (2010). The *Ita4h* locus modulates susceptibility to
648 mycobacterial infection in zebrafish and humans. *Cell* **140**, 717-730.

649 **Torok, M. E., Nguyen, D. B., Tran, T. H., Nguyen, T. B., Thwaites, G. E., Hoang, T. Q., Nguyen,**
650 **H. D., Tran, T. H., Nguyen, T. C., Hoang, H. T.** et al. (2011). Dexamethasone and long-term outcome
651 of tuberculous meningitis in Vietnamese adults and adolescents. *PLoS One* **6**, e27821.

652 **van der Goes, A., Hoekstra, K., van den Berg, T. K. and Dijkstra, C. D.** (2000).
653 Dexamethasone promotes phagocytosis and bacterial killing by human monocytes/macrophages in
654 vitro. *Journal of leukocyte biology* **67**, 801-807.

655 **van Leeuwen, L. M., van der Sar, A. M. and Bitter, W.** (2015). Animal models of tuberculosis:
656 zebrafish. *Cold Spring Harbor perspectives in medicine* **5**, a018580.

657 **Vernon-Roberts, B., Jessop, J. and Dore, J.** (1973). Effects of gold salts and prednisolone on
658 inflammatory cells. II. Suppression of inflammation and phagocytosis in the rat. *Annals of the*
659 *rheumatic diseases* **32**, 301.

660 **Wiysonge, C. S., Ntsekhe, M., Thabane, L., Volmink, J., Majombozi, D., Gumedze, F., Pandie,**
661 **S. and Mayosi, B. M.** (2017). Interventions for treating tuberculous pericarditis. *Cochrane Database*
662 *Syst Rev* **9**, Cd000526.

663 **World Health Organization.** (2019). Global tuberculosis report 2019. Geneva: World Health
664 Organization.

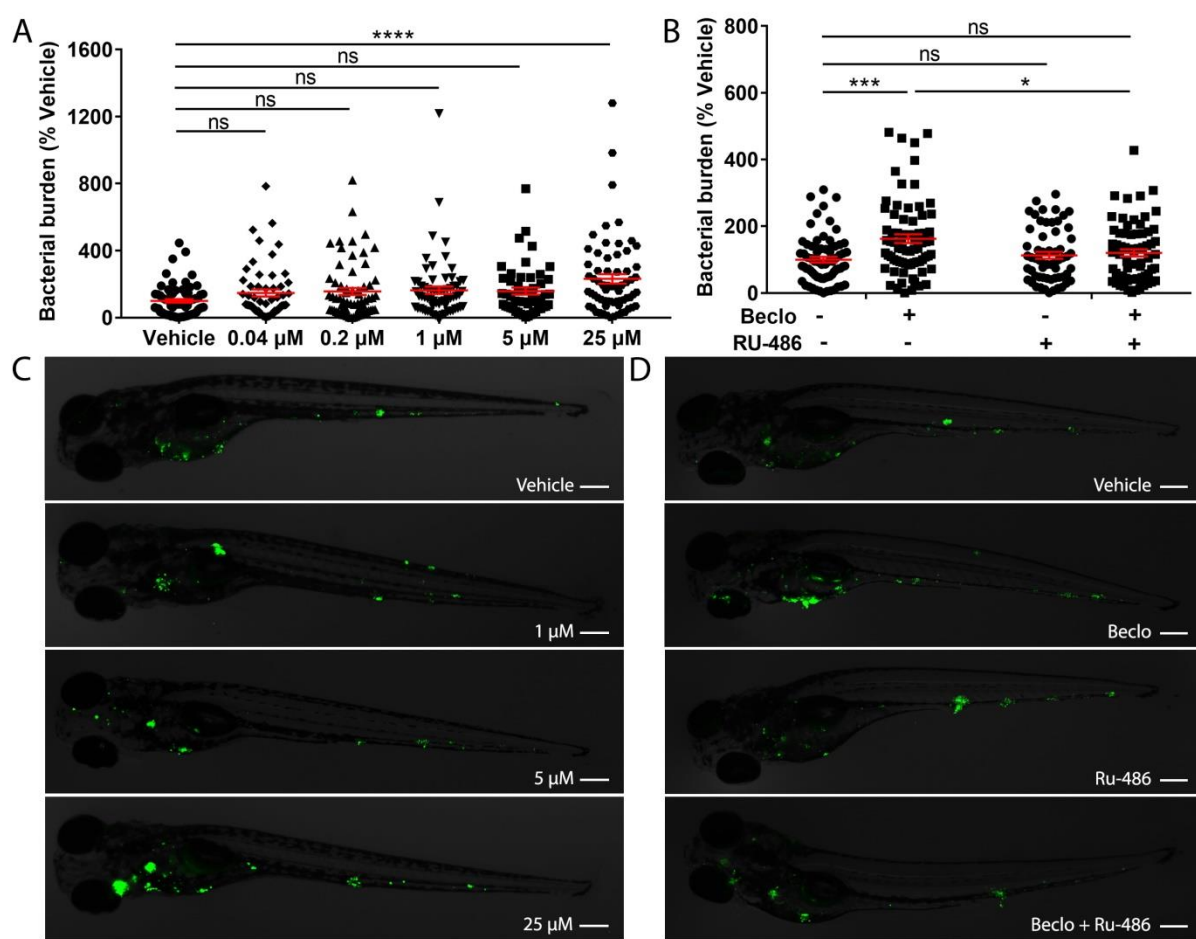
665 **Xie, Y., Tolmeijer, S., Oskam, J. M., Tonkens, T., Meijer, A. H. and Schaaf, M. J.** (2019).
666 Glucocorticoids inhibit macrophage differentiation towards a pro-inflammatory phenotype upon
667 wounding without affecting their migration. *Disease models & mechanisms* **12**, dmm037887.

668 **Zahuczky, G., Kristóf, E., Majai, G. and Fésüs, L.** (2011). Differentiation and Glucocorticoid
669 Regulated Apopto-Phagocytic Gene Expression Patterns in Human Macrophages. Role of Mertk in
670 Enhanced Phagocytosis. *PLoS One* **6**, e21349.

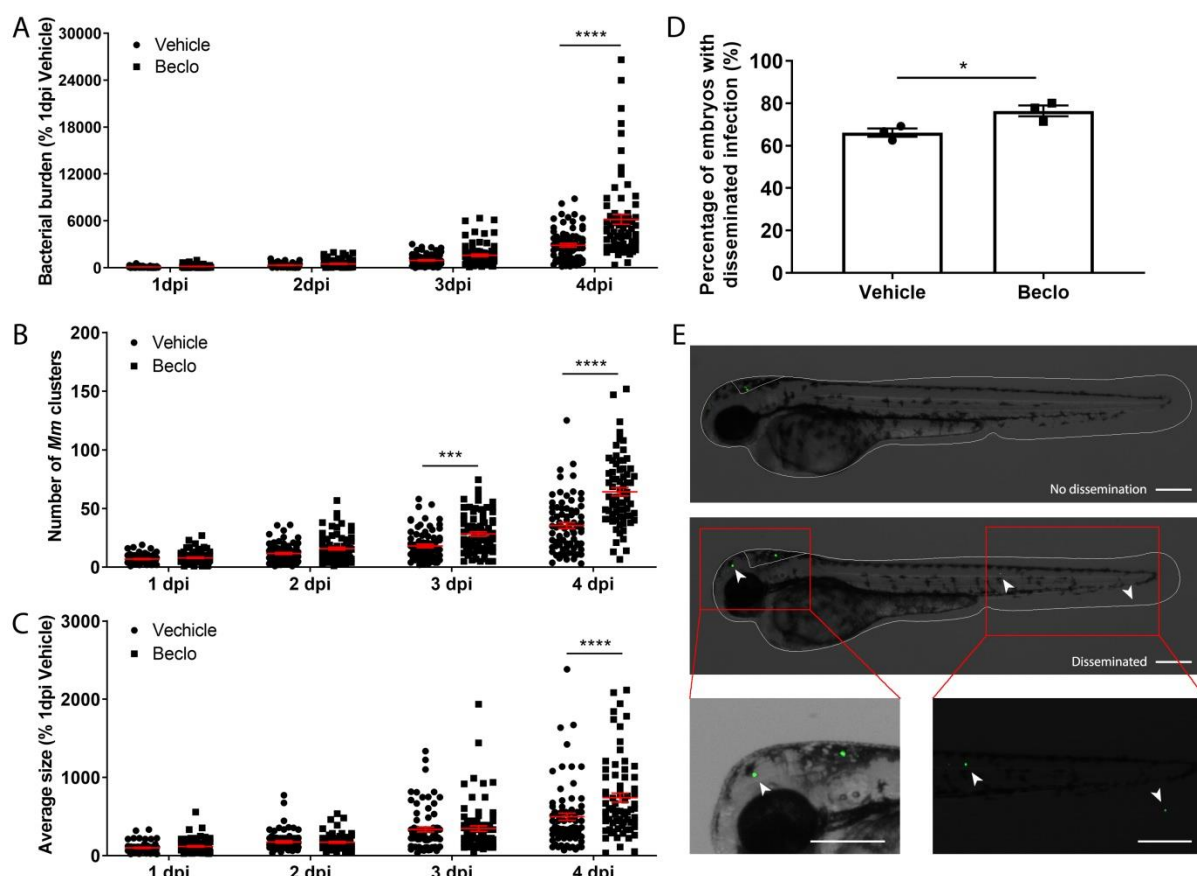
671 **Zakrzewska, A., Cui, C., Stockhammer, O. W., Benard, E. L., Spaink, H. P. and Meijer, A. H.**
672 (2010). Macrophage-specific gene functions in Spi1-directed innate immunity. *Blood* **116**, e1-11.

673 **Zhang, R., Varela, M., Forn-Cuni, G., Torraca, V., van der Vaart, M. and Meijer, A. H.** (2019).
674 Deficiency in the autophagy modulator Dram1 exacerbates pyroptotic cell death of Mycobacteria-
675 infected macrophages. *bioRxiv*, 599266.

676

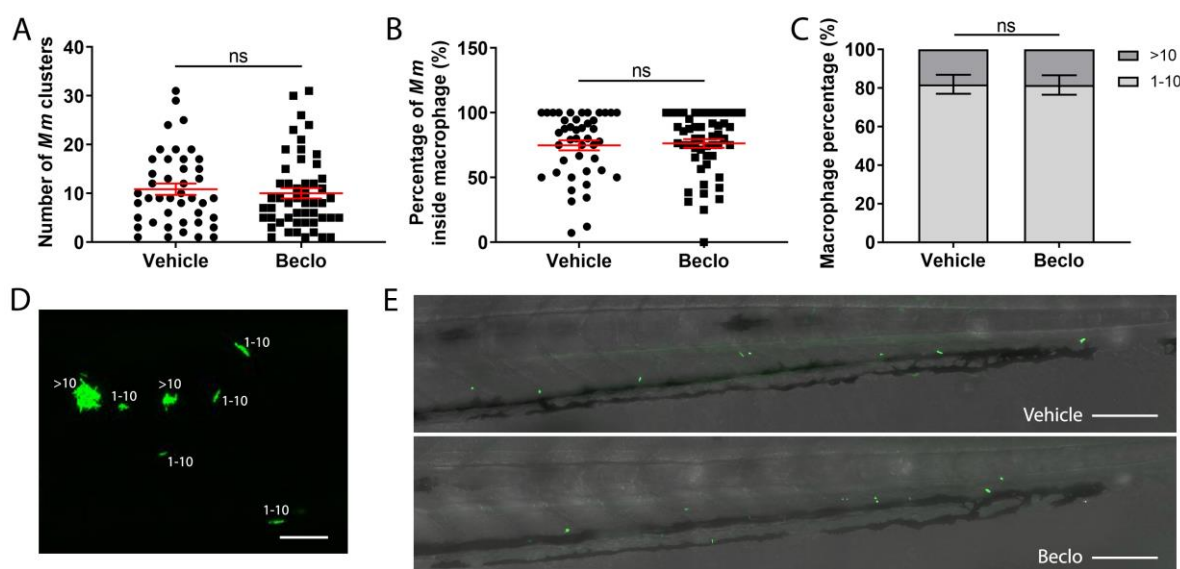


678 **Figure 1. Effect of beclomethasone on *Mm* infection burden in zebrafish.** A. Bacterial burden of
679 zebrafish larvae at four days after intravenous injection (at 28 hpf) of *Mm* and treatment with vehicle
680 or different concentrations of beclomethasone (beclo), started at 2 h before infection. Statistical
681 analysis by one-way ANOVA with Bonferroni's post hoc test revealed that the bacterial burden was
682 significantly increased in the group treated with 25 μ M beclomethasone, compared to the burden of
683 the vehicle-treated group. B. Effect of the GR antagonist RU-486 on the beclomethasone-induced
684 increase of the bacterial burden at 4 dpi. The bacterial burden was significantly increased by
685 beclomethasone (25 μ M) treatment and this increase was abolished in the presence of RU-486.
686 Statistical analysis was performed by two-way ANOVA with Tukey's post hoc test. In panels A and B,
687 each data point represents a single larva and the means \pm s.e.m. of data accumulated from three
688 independent experiments are shown in red. Statistical significance is indicated by: ns, non-significant;
689 * P<0.05; *** P<0.001; **** P<0.0001. C-D. Representative fluorescence microscopy images of *Mm*-
690 infected larvae at 4 days post infection (dpi), representing experimental groups presented in panels A
691 and B. Bacteria are shown in green. Scale bar = 200 μ m.



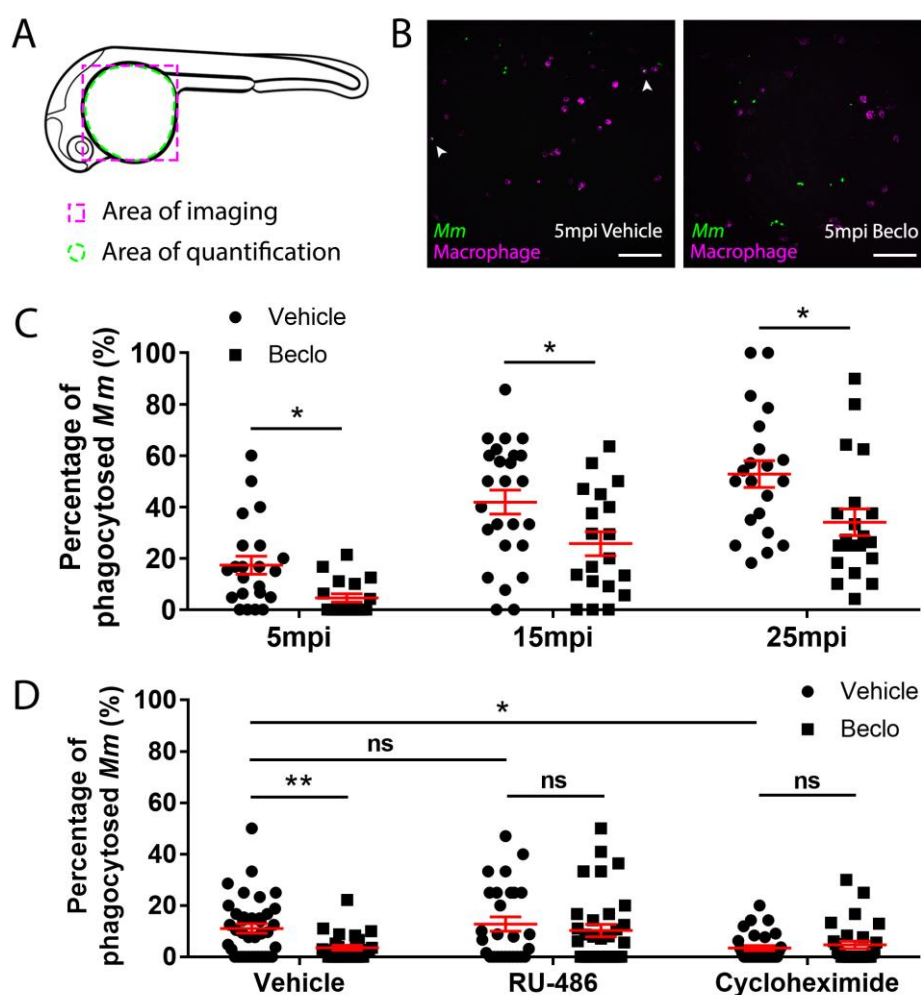
692

693 **Figure 2. Beclomethasone effects on *Mm* infection progression and bacterial dissemination.** A-C.
694 Bacterial burden (A), number of bacterial clusters (B) and the average size of bacterial clusters (C)
695 were determined at 1, 2, 3 and 4 dpi following intravenous *Mm* injection (28 hpf) and treatment with
696 vehicle or 25 μM beclomethasone, started at 2 h before infection. Significant increases due to the
697 beclomethasone treatment were observed for all parameters at 4 dpi. For the number of bacterial
698 clusters, the increase was also significant at 3 dpi. Statistical analysis was performed by two-way
699 ANOVA with Tukey's post hoc test. Each data point represents a single larva and the means ± s.e.m.
700 of data accumulated from three independent experiments are shown in red. Statistical significance is
701 indicated by: *** P<0.001; **** P<0.0001. D. Effect of beclomethasone on dissemination of *Mm* by
702 hindbrain ventricle injection. Hindbrain infections were performed at 28 hpf, and at 24 hours post
703 infection (hpi), a significantly increased percentage of larvae with disseminated *Mm* infection was
704 detected in the beclomethasone-treated group compared to the vehicle group. Statistical analysis
705 was performed by two-tailed t-test. Values shown are the means ± s.e.m. of three independent
706 experiments with a total sample size of 27 in the vehicle-treated group and 31 in the
707 beclomethasone-treated group. Statistical significance is indicated by: * P<0.05. E. Representative
708 images of embryos with and without dissemination of the infection upon hindbrain injection of *Mm*.
709 Scale bar = 200 μm.



710

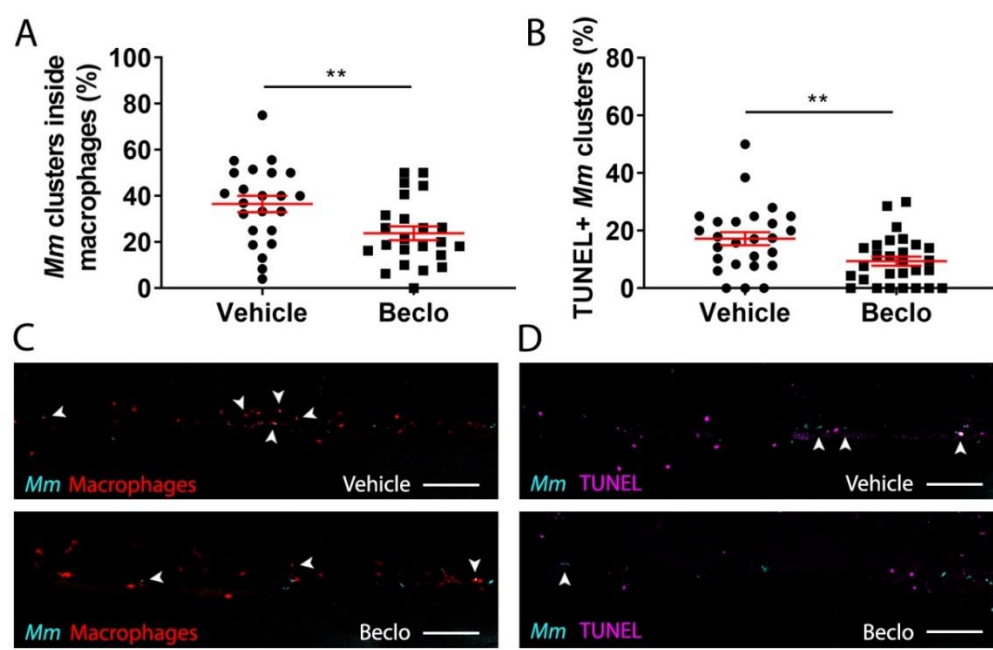
711 **Figure 3. Effect of beclomethasone on *Mm* Δ erp mutant bacterial growth.** A-C. The *Mm* Δ erp
712 mutant strain was injected intravenously at 28 hpf, and at 44 hpi the number of *Mm* clusters (A) and
713 the percentage of *Mm* inside macrophages (B), and the percentage of macrophages that contained 1-
714 10 or more than 10 bacteria (of all macrophages containing bacteria) (C) were determined. No
715 significant difference was observed between the vehicle- and beclomethasone-treated groups.
716 Statistical analysis was performed using two-tailed t-tests. Values shown are the means \pm s.e.m. of
717 three independent experiments, with each data point representing a single embryo. Statistical
718 significance is indicated by: ns, non-significant. D. Representative confocal microscopy image of *Mm*
719 Δ erp bacterial clusters (bacteria in green), indicated are clusters containing 1-10 bacteria and clusters
720 containing more than 10 bacteria. Scale bar = 20 μ m. E. Representative images of the tail regions of a
721 vehicle- and a beclomethasone-treated embryo infected with *Mm* Δ erp bacteria. Scale bar = 100 μ m.



722

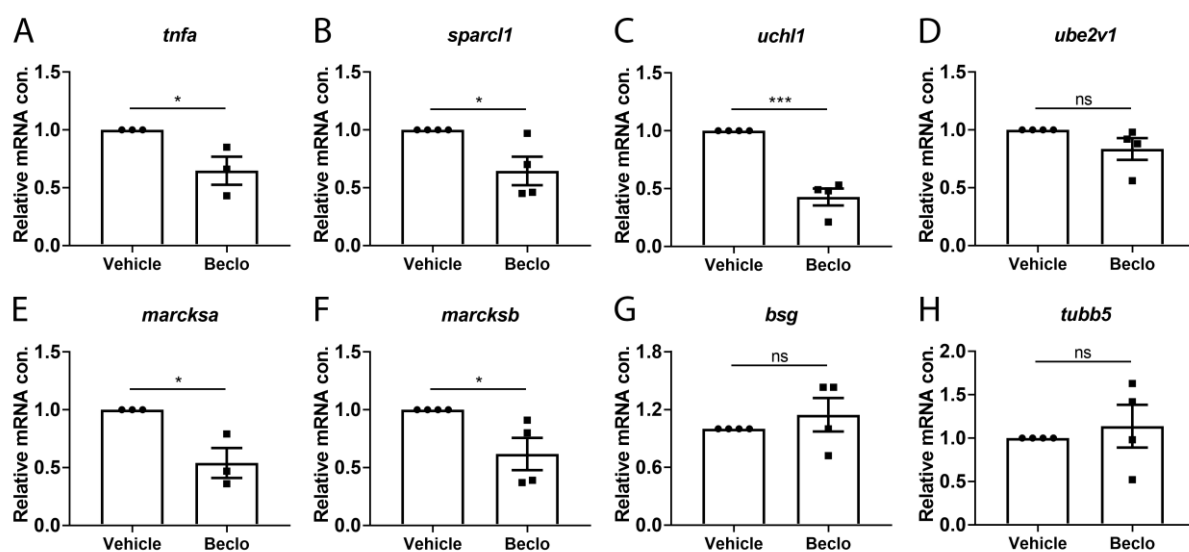
723 **Figure 4. Effect of beclomethasone on phagocytic activity of macrophages and its dependency on**
724 **Gr and de novo protein synthesis.** A. Schematic drawing of a zebrafish embryos at 28 hpf indicating
725 the areas of imaging (purple dashed box, used for representative images) and quantification (green
726 dashed circle) of *Mm* phagocytosis. B. Representative confocal microscopy images of embryos of the
727 *Tg(mpeg1:GFP)* line injected with *Mm* at 28 hpf. Images were taken of infected embryos that were
728 vehicle- or beclomethasone-treated at 5 minutes post infection (mpi). Macrophages are shown in
729 magenta, bacteria in green. Scale bar = 100 μ m. Arrowheads indicate bacterial clusters phagocytosed
730 by macrophages. C. Percentages of phagocytosed *Mm* clusters (of total number of *Mm* clusters) at 5,
731 15 and 25 mpi. Statistical analysis, performed by fitting data to a beta inflated regression with
732 Tukey's post hoc test, showed that beclomethasone decreased this percentage at all three time
733 points. D. Effects of RU-486 and cycloheximide on the beclomethasone-inhibited phagocytic activity.
734 Embryos were treated with vehicle or beclomethasone and received either a vehicle, RU-486 or
735 cycloheximide co-treatment two hours before injection of *Mm* at 28 hpf, and phagocytic activity was
736 determined at 5 mpi. The significant inhibitory effect of beclomethasone on phagocytosis was not
737 observed in the presence of RU-486. Cycloheximide, just like beclomethasone, significantly inhibited

738 the phagocytic activity, and the combined cycloheximide /beclomethasone treatment showed the
739 same level of inhibition. Statistical analysis was performed by fitting data to a beta inflated
740 regression with Tukey's post hoc test. In panels C and D, each data point represents a single embryo
741 and the means \pm s.e.m. of data accumulated from three independent experiments are shown in red.
742 Statistical significance is indicated by: ns, non-significant; * $P<0.05$; ** $P<0.01$.



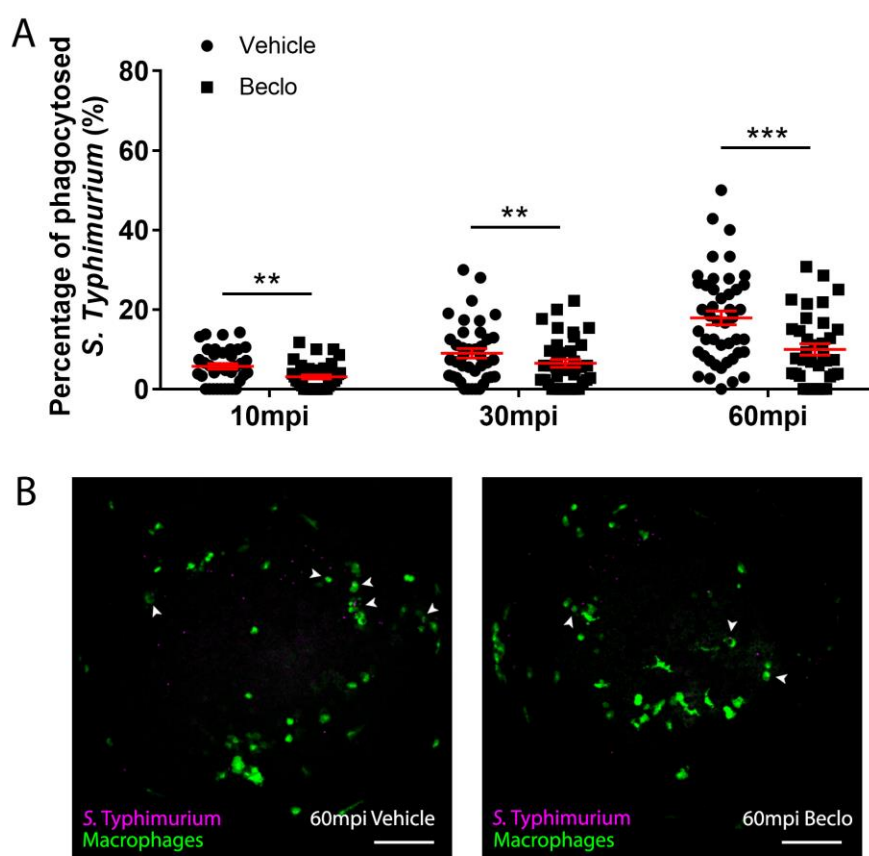
743

744 **Figure 5. Effect of beclomethasone on intracellular bacterial growth and cell death.** Infection was
745 performed in *Tg(mpeg1:mCherry-F)* embryos at 28 hpf, a TUNEL assay was performed at 48 hpi, and
746 the CHT region of the embryos was imaged using confocal microscopy. A. The percentage of *Mm*
747 clusters that were inside macrophages based on colocalization with the red fluorescent signal from
748 mCherry. Statistical analysis was performed by two-tailed t-test. In the beclomethasone-treated
749 group, the percentage of *Mm* clusters inside macrophages was significantly lower compared to the
750 vehicle-treated group. B. The percentage of TUNEL-positive *Mm* clusters. Statistical analysis by two-
751 tailed t-test showed that the beclomethasone-treated group had a significantly lower percentage of
752 TUNEL+ *Mm* clusters. In panels A and B, each data point represents a single embryo and the means ±
753 s.e.m. of data accumulated from three independent experiments are shown in red. Statistical
754 significance is indicated by: ** P<0.01. C. Representative confocal microscopy images of macrophage
755 phagocytosis. Bacteria are shown in blue and macrophages in red. Arrowheads indicate intracellular
756 bacterial clusters. Scale bar = 100 μm. D. Representative confocal microscopy images of cell death
757 (TUNEL+ cells in magenta) and *Mm* infection (bacteria in blue). Arrowheads indicate bacterial clusters
758 overlapping with TUNEL+ cells. Scale bar = 100 μm.



759

760 **Figure 6. Effect of beclomethasone on gene expression levels in FACS-sorted macrophages.** At 28
761 hpf, *Tg(mpeg1:mCherry-F)* embryos were treated with vehicle or beclomethasone for two hours,
762 after which macrophages were isolated by FACS sorting. Gene expression levels were determined in
763 the sorted cells by qPCR for *tnfa* (A), *sparcl1* (B), *uchl1* (C), *ube2v1* (D), *marcksa* (E), *marcksb* (F), *bsg*
764 (G) and *tubb5* (H). Statistical analysis by two-tailed t-test showed that the levels of *tnfa*, *sparcl1*,
765 *uchl1*, *marcksa* and *marcksb* expression were significantly inhibited by beclomethasone treatment.
766 Data shown are the means \pm s.e.m. of three or four independent experiments, and markers show
767 averages of individual experiments. Statistical significance is indicated by: ns, non-significant; *
768 P<0.05; *** P<0.001.



769

770 **Figure 7. Effect of beclomethasone on phagocytosis of *Salmonella* Typhimurium.** At 28 hpf
771 *Tg(mpeg1:GFP)* embryos (vehicle- or beclomethasone-treated) were infected with *S. Typhimurium*
772 through intravenous injection. At 10, 30, and 60 mpi, confocal microscopy images were taken of the
773 yolk area, as indicated in Figure 4A, and the macrophage phagocytic capacity was determined. A.
774 Percentage of phagocytosed *S. Typhimurium* at 10, 30 and 60 mpi. Statistical analysis, performed by
775 fitting data to a beta inflated regression with Tukey's post hoc test, showed that the phagocytic
776 activity of macrophages was significantly inhibited by beclomethasone treatment at 60 mpi, and not
777 at other time points. Each data point represents a single embryo and the means \pm s.e.m. of data
778 accumulated from three independent experiments are shown in red. Statistical significance is
779 indicated by: ns, non-significant; **** P<0.0001. B. Representative confocal microscopy images of
780 infected vehicle- and beclomethasone-treated individuals at 60 mpi. Bacteria are shown in magenta,
781 macrophages in green. Arrowheads indicate bacteria phagocytosed by macrophages. Scale bar = 100
782 μ m.